

# Grain Boundary Diffusion in Copper under Tensile Stress

Kevin M. Crosby

*Departments of Physics and Computer Science, Carthage College, Kenosha, WI 53158*

(Dated: June 30, 2003)

Stress enhanced self-diffusion of Copper on the  $\Sigma 3$  twin grain boundary was examined with molecular dynamics simulations. The presence of uniaxial tensile stress results in a significant reduction in activation energy for grain-boundary self-diffusion of magnitude 5 eV per unit strain. Using a theoretical model of point defect formation and diffusion, the functional dependence of the effective activation energy  $Q$  on uniaxial tensile strain  $\epsilon$  is shown to be described by  $Q(\epsilon) = Q_0 - E_0 V^* \epsilon$  where  $E_0$  is the zero-temperature Young's modulus and  $V^*$  is an effective activation volume. The simulation data agree well with this model and comparison between data and model suggests that  $V^* = 0.6\Omega$  where  $\Omega$  is the atomic volume.  $V^*/\Omega = 0.6$  is consistent with a vacancy-dominated diffusion mechanism.

## I. INTRODUCTION

Studies of failure mechanisms in nano-structured metallic interconnects show that diffusion near grain boundaries (GBs) plays a critical role in initiation of destructive mass-transport.<sup>1,2,3</sup> For example, electromigration failure of poly-crystalline aluminum and copper interconnects is initiated predominantly at grain boundaries and triple points. In accord with these phenomenological observations are measured and calculated activation energies for self-diffusion that are approximately one-third to one-half the corresponding bulk activation energies.<sup>4</sup> Typically metallic interconnects are under large tensile strains due to both the deposition process and the interaction with an underlying substrate or overlying passivation layer. Metallic interconnects in very- and ultra-large-scale-integrated circuit (VLSI/ULSI) applications can experience tensile stresses in excess of several hundred MPa resulting in strains on the order of several hundredths of a percent. While it is well known that external tensile strain enhances diffusivity in bulk materials, there have been relatively few experimental or computational investigations of diffusion in strained metals despite the technological significance of the problem.

Due to its use in nano-scale interconnect materials, the structural properties and self-diffusion mechanisms in copper near GBs have received considerable attention.<sup>5,6,7,8,9,10</sup> Several experiments on the microstructure of copper thin films suggest that the  $\Sigma 3$  coherent twin grain boundary accounts for roughly 42% of all coincident-site-lattice (CSL) boundaries in as-deposited copper thin films.<sup>11</sup> CSL boundaries together represent the majority of GB geometries in polycrystalline copper. Further, calculations of GB surface energies show that the  $\Sigma 3$  boundary has a markedly lower energy than all but the  $\Sigma 7$  boundary.<sup>12</sup> While, compared to other CSL boundaries, defect mobility is relatively low in the  $\Sigma 3$  GB, the large number of such boundaries present in copper thin films motivates the study of diffusion near these structures.

Bulk self-diffusion in metals may be considerably simpler than diffusion near GBs. Sandberg *et al.* have recently demonstrated that monovacancies are the only ac-

tive contributors to bulk diffusion in aluminum at all temperatures up to the melting point.<sup>13</sup> The situation near GBs is far from resolved, however, and is certainly more complicated than that in the bulk. Sorensen *et al.* established that symmetric tilt GBs support both vacancy and interstitial-mediated diffusion at low temperatures, while at elevated temperatures, more complex defect interactions such as Frenkel pairs and even ring mechanisms contribute to GB diffusion.<sup>6</sup> Recently, Suzuki and Mishin demonstrated that vacancy and interstitial mechanisms can have comparable formation energies in symmetric tilt boundaries in copper.<sup>14</sup> There is also ample experimental evidence of complex, cooperative motion of large numbers of atoms in both twist and tilt GBs in thin Au films at high temperature.<sup>15</sup>

Nomura and Adams have extensively studied diffusion mechanisms in and near both symmetric tilt and pure twist GBs in copper.<sup>4</sup> Assuming only a vacancy mechanism for diffusion in twist boundaries, Nomura and Adams found that diffusion at low temperatures is dominated by migration along the screw dislocations comprising high angle twist boundaries, while high temperature diffusion occurred primarily through the bulk. Nomura and others have also established that vacancies are strongly bound to the GB itself so that vacancy diffusion is primarily restricted to the plane defined by the GB.

Because of the constraining geometry of the twin boundary studied in the present work, it is unlikely that interstitials and more complex defects such as Frenkel pairs contribute significantly to diffusion on the  $\Sigma 3$  GB at low temperatures.<sup>5</sup> At elevated temperatures, however, defect concentrations may be high enough that interactions between point defects may contribute to diffusion near the GB. While appropriate mechanisms have been tentatively identified for bulk diffusion, mechanisms for diffusion near grain boundaries have not been clearly established.<sup>16</sup>

As a computational problem, diffusion near GBs in copper has been examined in the context of molecular dynamics (MD), molecular statics (MS), and, more recently, kinetic Monte Carlo (KMC) models.<sup>4,5,6,7</sup> Because MD evolves the atomic lattice directly according to a specified potential, all migration pathways and diffusion

mechanisms are allowed. For this reason, MD is useful in identifying the kinetics of defect formation, differentiating between diffusion through vacancy and interstitial migration when, as is the case for GB diffusion, a dominant mechanism has not been identified.

Typically, MD simulations are limited to time scales on the order of nano-seconds, often too short to reliably extrapolate diffusion constants at the relatively low (in terms of bulk melting temperatures) operating temperatures of copper interconnects in micro-electronics technologies. As a result, an accurate estimation of activation energies for self-diffusion is difficult. Conversely, the MS and KMC methods and other approaches involving the coupled application of Monte Carlo and molecular statics approaches requires an *a priori* knowledge of defect types, concentrations, and jump frequencies, but overcomes the short-time scale limitations of direct MD simulations. Recently, hybrid approaches have been demonstrated that combine the strengths of each simulation technique to more reliably estimate diffusion properties in metals.<sup>6</sup>

In this paper, I report on the use of MD to determine activation energies as a function of static lattice-strain for self-diffusion on the  $\Sigma 3$  coherent twin grain boundary in copper. In Sec. II, the details of the computational model are developed, and fundamental elastic properties of the simulated crystal are calculated and compared with existing data to validate the bulk mechanical behavior of the computational model. A theoretical framework for the diffusion data obtained in the simulations is presented in Sec. III, while in Sec. IV, the activation energy data and other relevant results are presented and interpreted within the theoretical framework of Sec. III. Finally, a discussion of the results in the context of existing and future experimental and numerical work is presented in Sec. V.

## II. COMPUTATIONAL MODEL

Molecular dynamics simulations using potentials derived from the embedded-atom model (EAM) are well-known to accurately account for the behaviors of metals, particularly near surfaces and point defects where other semi-classical potentials fail. The accuracy of several of these potentials in accounting for the thermodynamics and energetics of extended defects such as grain boundaries has recently been established as well.<sup>17</sup> The simulations reported here make use of EAM potentials for copper published by Johnson.<sup>18</sup> The potential has been modified for a smooth cut-off and to better match bulk mechanical properties of copper.<sup>19</sup> The MD time-step is 0.9 fs, and each simulation is carried out for at least 1.2 ns, with lower temperature simulations run for up to 2.2 ns to obtain reasonable diffusion statistics.

A simulation cell with dimensions  $20\text{\AA} \times 40\text{\AA} \times 40\text{\AA}$ , consisting of roughly 128,000 atoms is sliced in half such that the slice-plane separates two  $\{111\}$  crystal faces

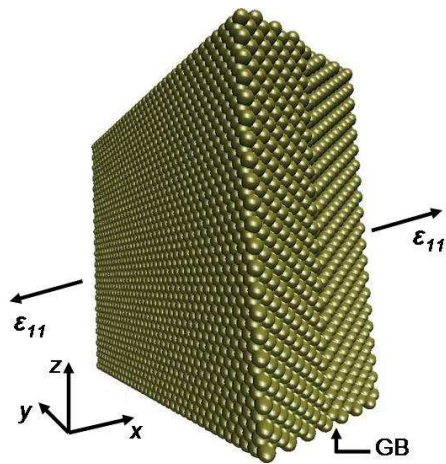


FIG. 1: A  $12\text{\AA} \times 25\text{\AA} \times 25\text{\AA}$  section of the full simulation cell with a  $\Sigma 3$  GB on the central (111) plane. A tensile strain is applied along the external coordinate direction  $\mathbf{x}$  which is aligned along the  $\langle 111 \rangle$  crystallographic direction.

of the copper lattice. The slice plane defines a grain boundary of area  $1600\text{\AA}^2$ . To generate the coherent twin boundary, one side of the crystal is rotated by  $60^\circ$  about the  $\langle 111 \rangle$  axis. The geometry is illustrated in Fig. 1. Periodic boundary conditions are applied to the faces of the crystal normal to the GB, while the two surfaces parallel to the GB are free. As indicated in Fig. 1, the external coordinate direction  $\mathbf{x}$  is aligned with the crystallographic direction  $\langle 111 \rangle$ .

To find the energetically favorable separation of the two crystallites defining the GB, Monte Carlo relaxation is carried out to optimize the separation between the two crystallites and a minimum-energy separation is obtained for each temperature. The equilibrium lattice constant is established through short MD calculations which search for a minimum in internal stress as the lattice constant is varied at a fixed temperature.

For temperatures in the range  $0.44T_m < T < 0.74T_m$ , where  $T_m = 1356\text{K}$  is the experimental bulk melting temperature of copper, the Young's modulus,  $E = \sigma_{11}/\epsilon_{11}$  and the Poisson ratio,  $\nu = \epsilon_{22}/\epsilon_{11}$  are evaluated from the elastic coefficients  $C_{11}$  and  $C_{12}$ . The  $C_{ij}$  are obtained from the ensemble averages of fluctuations in the stress tensor using the method of Ref. 20. Poisson's ratio  $\nu$  for tension in the  $\mathbf{x}$  direction is relatively insensitive to temperature and takes the value  $\nu = 0.31 \pm 0.02$  for all simulations reported here.

The calculated temperature dependence of the Young's modulus  $E(T)$  is shown in Fig. 2 and obeys the phenomenological relation

$$E(T) = E_0(1 - \gamma T/T_m) \quad (1)$$

for temperatures  $T \leq 0.74T_m$  where  $E_0 = 116\text{ GPa}$  is the zero-temperature modulus, and  $\gamma \approx 0.55$ . Çağın *et al.* calculate the elastic constant  $C_{11}$  as a function of temperature for copper.<sup>21</sup> Their data is in excellent

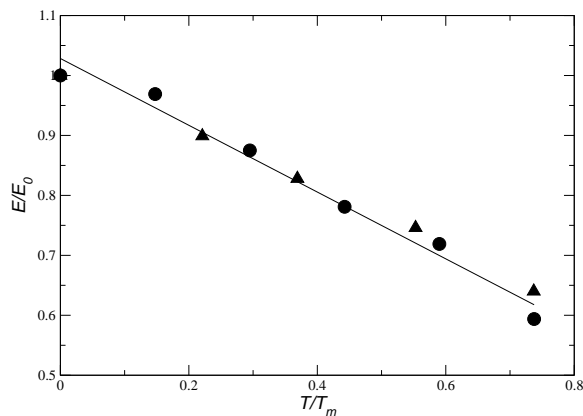


FIG. 2: The temperature dependence of the Young's modulus  $E \equiv \sigma_{11}/\epsilon_{11}$  for uniaxial tension in units of the zero temperature modulus  $E_0 = 116$  GPa (circles). The solid line is a linear regression fit with slope  $-0.55$ . The triangles are data obtained from Ref.<sup>21</sup> with  $E_0 = 127$  GPa. Both data sets are well described by  $E(T) = E_0(1 - \gamma T/T_m)$  with  $\gamma = 0.55$  and  $T_m = 1356$  K.

agreement with Eq. 1 when one applies the relation  $C_{11} = (1 - \nu)E/(1 + \nu)(1 - 2\nu)$  to obtain the Young's modulus for uniaxial tension along the  $x$  direction from the data in Ref.<sup>21</sup>.

To study diffusion under strain, the lattice is equilibrated at each target temperature using Monte Carlo relaxation. A strain rate of  $\dot{\epsilon} = 10^{-4}$  ps $^{-1}$  is applied to the (111) faces of the lattice until a desired average internal static strain  $\epsilon_{11}$  is reached. Diffusivities are calculated from the mean-square displacement of atoms in and near the GB according to

$$D_\alpha = \frac{1}{6t} \langle r_\alpha^2(t) \rangle \quad (2)$$

where  $r_\alpha(t)$  is the  $\alpha$  component of the atomic displacement vector on the GB plane at time  $t$ , and the average is over all atoms originating in either of the two atomic planes defining the grain boundary. The diffusivity  $D_\parallel$  parallel to the GB is computed at temperatures ranging from  $0.44T_m$  to  $0.74T_m$  for a range of static strains from 0 to 0.07. The maximum corresponding stresses are on the order of a few GPa. From the diffusivity data, Arrhenius plots are constructed and the effective activation energy is computed at each value of the static strain  $\epsilon$ .

### III. DIFFUSION UNDER UNIAXIAL TENSILE STRAIN

In the simulations reported here, the copper crystal is under uniaxial tension  $\sigma_{11}$  due to a static strain applied at the (111) faces as shown in Fig. 1. The lattice strain is given by  $\epsilon_{11} = \epsilon$ ,  $\epsilon_{22} = \epsilon_{33} = -\nu\epsilon$ , and all other  $\epsilon_{ij} = 0$ . Diffusion in the plane of the GB is characterized by the

diffusivity components  $D_{12}$  and  $D_{13}$  which we can take to be equal:  $D_\parallel \equiv D_{12} = D_{13}$ . Transport normal to the GB is described by the diffusion constant  $D_{11}$ . In the simulations reported in this paper, we have adopted a very narrow definition of the grain boundary region as consisting of just the two atomic planes adjacent to the interface. For this reason, we are interested in the diffusivity  $D_\parallel$  within the grain boundary plane  $y - z$ , and we anticipate that  $D_{11}$  will reflect bulk diffusivity that is not of interest here.

Experimentally, the effect of tensile strain  $\epsilon$  on diffusivity  $D$  has been characterized by an effective reduction of the activation energy for diffusion by the amount<sup>22,23</sup>

$$Q' = -kT \frac{\partial \ln D}{\partial \epsilon}. \quad (3)$$

Aziz has provided a rigorous theoretical foundation for the empirical result of Eq. 3.<sup>24,25</sup> We make use of the theory in Ref.<sup>25</sup> in what follows.

After Aziz, we consider the components of the diffusivity tensor  $\mathbf{D}$  to be proportional to the product of the defect concentration  $C(\boldsymbol{\sigma})$  and appropriate component of the mobility tensor  $\mathbf{M}(\boldsymbol{\sigma})$  of point defects in the lattice. Here,  $\boldsymbol{\sigma}$  is the spatially uniform stress tensor with components  $\sigma_{ij}$ . The equilibrium concentration of defects is related to the stress-free concentration  $C(0)$  by

$$\frac{C(\boldsymbol{\sigma})}{C(0)} = \frac{\exp(\boldsymbol{\sigma} \cdot \mathbf{V}^f)}{kT}. \quad (4)$$

The formation strain tensor  $\mathbf{V}^f$  depends on the defect mechanism, as well as on the location of the defect source and represents the volume changes due to the formation of a defect. Experimentally, only certain components of  $\mathbf{V}^f$  are accessible. In the case of hydrostatic stresses, the formation volume  $V^f \equiv \text{Tr} \mathbf{V}^f$  is measured.

Consider point defects forming on or near the GB plane. A vacancy (interstitial) defect initially increases (decreases) the sample volume by one atomic volume unit  $\Omega$  on the (111) face which is normal to the external coordinate direction  $\mathbf{x}$ . Subsequent to a vacancy (interstitial) formation, the lattice relaxes around the defect, contracting (expanding) around the vacancy (interstitial). The resulting change in volume is characterized by the relaxation volume  $V^r$  which is negative (positive) for vacancy (interstitial) defects. The defect formation tensor is then given by

$$\mathbf{v}^f = \pm \Omega \begin{pmatrix} 1 & 0 & 0 \\ 0 & 0 & 0 \\ 0 & 0 & 0 \end{pmatrix} + \frac{V^r}{3} \begin{pmatrix} 1 & 0 & 0 \\ 0 & 1 & 0 \\ 0 & 0 & 1 \end{pmatrix} \quad (5)$$

where  $+$  ( $-$ ) sign is for vacancy (interstitial) formation.

The directional dependence of the diffusivity is contained in the mobility tensor,  $\mathbf{M}$ . The defect mobility is also stress dependent, and its contribution to the self-diffusivity is through the migration strain tensor  $\mathbf{V}^m$ . Diffusion in the plane of the grain boundary depends on

the mobility  $\mathbf{M}_{\parallel} \equiv \mathbf{M}_{12} \approx \mathbf{M}_{13}$  according to

$$\frac{\mathbf{M}_{\parallel}(\boldsymbol{\sigma})}{\mathbf{M}_{\parallel}(0)} = \frac{\exp(\boldsymbol{\sigma} \cdot \mathbf{V}_{\parallel}^m)}{kT} \quad (6)$$

where  $\mathbf{V}_{\parallel}^m$  is the migration strain tensor in the plane of the GB and the migration volume  $V^m = \text{Tr} \mathbf{V}^m$  represents the change in volume of the lattice after the defect has reached the saddle point in its migration path.

From Equations 4 and 6, the stress dependence of  $D_{\parallel}$  is given by

$$\ln \frac{D_{\parallel}(\boldsymbol{\sigma})}{D_{\parallel}(0)} = \frac{\boldsymbol{\sigma} \cdot (\mathbf{V}^f + \mathbf{V}_{\parallel}^m)}{kT}. \quad (7)$$

For the simple tension condition used in our simulations, the stress tensor has a single non-zero component,  $\sigma_{11} = E\epsilon$  where  $\epsilon$  is the magnitude of the strain along the  $x$  direction:  $\epsilon_{11} = \epsilon > 0$ . Under uniaxial tension in the  $\mathbf{x}$  direction, Eq. 7 becomes

$$\ln \frac{D_{\parallel}(\epsilon)}{D_{\parallel}(0)} = \frac{E(\pm\Omega + V^r/3 + V_{xx}^m)\epsilon}{kT}, \quad (8)$$

where  $V_{xx}^m$  is the dimension change in the  $\mathbf{x}$  direction upon defect migration to its saddle point.

In an unstrained lattice, the usual Arrhenius form for the diffusivity,

$$\ln \frac{D}{D_0} = -\frac{Q_0}{kT} \quad (9)$$

holds, where  $D_0$  is a material constant, and  $Q_0$  is the activation energy for self-diffusion in the unstrained lattice.  $Q_0$  is the sum of a defect formation energy  $Q_0^f$  and a migration energy,  $Q_0^m$ . It is clear from Eqns. 8 and 9 that the effective activation energy for the case of simple tension considered here is

$$Q(\epsilon) = Q_0 - EV^*\epsilon, \quad (10)$$

where

$$V^* \equiv \pm\Omega + V^r/3 + V_{xx}^m. \quad (11)$$

The effect of tensile strain is to reduce the effective activation energy for self-diffusion by the amount  $EV^*$  per unit strain.

High-temperature elastic softening of the copper crystal does not change the fundamental Arrhenius analysis of diffusion coefficients. Combining Eqns. 1, 7, and 11, we find the Diffusion coefficient is still of Arrhenius form:

$$\ln \frac{D_{\parallel}(\epsilon)}{\tilde{D}_{\parallel 0}(\epsilon)} = -\frac{Q(\epsilon)}{kT} \quad (12)$$

where  $\tilde{D}_{\parallel 0}(\epsilon) = D_{\parallel 0} e^{-\gamma E_0 V^* \epsilon / kT_m}$ , and  $D_{\parallel 0}$  is a material constant. The strain-dependent activation energy  $Q(\epsilon)$  in Eq. 12 is given by Eq. 10 with  $E$  replaced by  $E_0$ . The functional form of the effective activation energy is unchanged by elastic softening, and the usual Arrhenius analysis is still appropriate for the determination of diffusivities and activation energies.

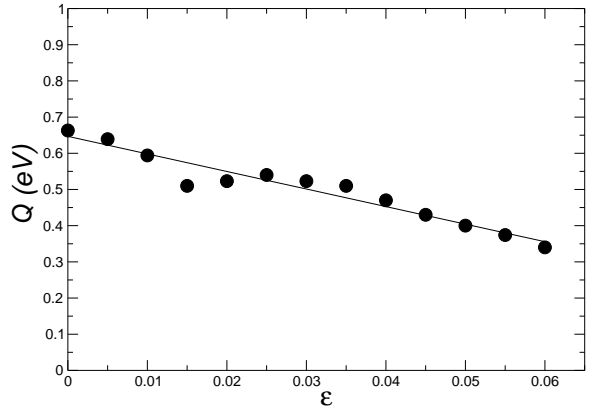


FIG. 3: The effective activation energy is plotted against the strain  $\epsilon_{11} = \epsilon$ . The solid line is a linear regression fit with slope 4.9 eV.

#### IV. SIMULATION RESULTS

The essential result of the MD simulations is the functional dependence of effective activation energy on lattice strain for diffusion on the GB plane. The function  $Q(\epsilon)$  is obtained from the Arrhenius plots of Diffusivity  $D_{\parallel}$  vs. inverse temperature. This dependence is illustrated in Fig. 3. The solid line in Fig. 3 is a linear regression fit to the data of the form  $Q(\epsilon) = 0.65\text{eV} - 4.9\text{eV}\epsilon$ . While experimental data with conditions similar to those simulated here are not known to us, there are some general observations and comparisons that can be made with respect to the functional dependence of activation energy on strain. As expected, the zero-strain activation energy  $Q(0) = 0.65$  eV is higher than that for most tilt boundaries in copper, but significantly lower than the bulk activation energy of 1.3 eV for self-diffusion in copper.

To place our data in the context of the analysis in Sec. III, let us compare the slope of the  $Q(\epsilon)$  data in Fig. 3 with the predicted slope  $E_0 V^*$  (Eq. 10). With  $E_0 = 116$  GPa, we find  $V^* = 0.6\Omega$ , where  $\Omega = 1.2 \times 10^{-29} \text{m}^3$  is the atomic volume for fcc-copper. While there is no experimental data with which to compare the value of  $V^*$ ,  $V^*/\Omega = 0.6$  is consistent with vacancy-dominated diffusion and inconsistent with an interstitial-type mechanism. This conclusion is based on the assumption that the migration volume contribution  $V_{xx}^*$  is negligible in comparison to the other volume terms in Eq. 11. Assuming a vacancy mechanism in Eq. 11, we find that the relaxation volume satisfies  $V^r/\Omega = -1.2$ , while the assumption of a pure interstitial mechanism results in  $V^r/\Omega = +4.8$ . The latter value is implausibly large, and we conclude that simple vacancies represent the dominant point defects in the GB.

## V. DISCUSSION

To estimate the technological significance of strain in interconnect device applications, consider that tensile stresses in copper interconnects are typically on the order of several hundred MPa, and the resulting strains depend on the crystallographic direction of the applied stress, but are on the order of  $10^{-3}$ . A reduction in effective activation energy of  $\approx 5$  eV per unit strain suggests that the strain effect is of order  $10^{-2}$  eV, effectively doubling diffusivity at room temperature. While experimental diffusivity measurements can be uncertain to within orders of magnitude, static intrinsic strains typical of modern interconnect materials may significantly enhance diffusion near GBs in these materials.

Any attempt to calculate activation energies from diffusion constants obtained with MD simulations is risky,

in that the simulation time-scale may be shorter than the time taken for the defect concentration to reach equilibrium. However, the zero-strain activation energy  $Q_0 = 0.65$  eV reported in this paper is within the range of values obtained by others for diffusion on a variety of GBs using molecular statics and assumptions about the dominant defect mechanism.<sup>4</sup> The evidence for a dominant vacancy-type mechanism is also consistent with several previous studies of defect formation on coherent twin GBs.

Future computational work on grain boundary diffusion in copper will focus on measurements of  $V^*$  for other technologically important GBs such as the  $\Sigma 7$  GB family. Like the  $\Sigma 3$  twin,  $\Sigma 7$  GBs are found in relatively high numbers in as-deposited copper thin films, but typically have significantly higher defect mobility than the  $\Sigma 3$  GB.

- 
- <sup>1</sup> M. R. Achter and R. Smoluchowski, *J. Appl. Phys.* **22**, 1260 (1951).
- <sup>2</sup> R. S. Barnes, *Nature* **166**, 1032 (1950).
- <sup>3</sup> D. Turnbull, *Phys. Rev.* **76**, 417A (1949).
- <sup>4</sup> M. Nomura and J. Adams, *J. Mater. Res.* **7**, 3202 (1992).
- <sup>5</sup> M. Nomura, S. Lee, and J. Adams, *J. Mater. Res.* **6**, 1 (1991).
- <sup>6</sup> M. Sorensen, Y. Mishin, and A. Voter, *Phys. Rev. B* **62**, 3658 (2000).
- <sup>7</sup> H. Van Swygenhoven, D. Farakas, and A. Caro, *Phys. Rev. B* **62**, 831 (2000).
- <sup>8</sup> M. Nomura and J. Adams, *J. Mater. Res.*, **10**, 2916 (1995).
- <sup>9</sup> Q. Ma and R. W. Balluffi, *Acta Metall. Mater.* **41**, 133 (1993).
- <sup>10</sup> J. Sommer, Chr. Herzig, T. Muschik, and W. Gust, *Acta Metall. Mater.* **43**, 1099 (1995).
- <sup>11</sup> *Grain size, grain boundary and quantitative texture analysis of a Cu thin film* (2003), from HKL Technologies Application Notes: [http://www.hkltechnology.com//applic\\_notes//app7.pdf](http://www.hkltechnology.com//applic_notes//app7.pdf).
- <sup>12</sup> A. Rollett, *Mat. Sci. Forum: Proceedings of the 8th International Conference on Aluminum and its Alloys* **396**, 593 (2002).
- <sup>13</sup> N. Sandberg, B. Magyari-Köpe, and T. Mattsson, *Phys. Rev. Lett.* **89**, 65901 (2002).
- <sup>14</sup> A. Suzuki and Y. Mishin, *Interface Science* **11**, 131 (2003).
- <sup>15</sup> K. L. Merkle, L. J. Thompson, and F. Phillipp, *Phys. Rev. Lett.* **88**, 225501 (2002).
- <sup>16</sup> D. Farakas, *J. Phys.: Condens. Matter* **12**, R497 (2000).
- <sup>17</sup> C. Liu and S. J. Plimpton, *J. Mater. Res.* **10**, 1589 (1995).
- <sup>18</sup> R. A. Johnson, *Phys. Rev. B* **37**, 3924 (1988).
- <sup>19</sup> D. J. Oh and R. A. Johnson, *J. Mater. Res.* **3**, 471 (1996).
- <sup>20</sup> J. Ray and A. Rahman, *J. Chem. Phys.* **80**, 4243 (1985).
- <sup>21</sup> T. Çağın, G. Dereli, M. Uludoğan, and M. Tomak, *Phys. Rev. B* **59**, 3468 (1999).
- <sup>22</sup> M. Aziz, *Defect and Diffusion Forum* **153-155**, 1 (1998).
- <sup>23</sup> N. Moriya, L.C. Feldman, H. S. Luftman, C. A. King, J. Bevk, and B. Freer, *Phys. Rev. Lett.* **71**, 883 (1993).
- <sup>24</sup> M. J. Aziz, P. C. Sabin, and G. Lu, *Phys. Rev. B* **44**, 9812 (1991).
- <sup>25</sup> M. J. Aziz, *Appl. Phys. Lett.* **70**, 26 (1997).